PROCEEDINGS OF SCIENCE

Measurement of the very rare $K^+ \to \pi^+ \nu\bar{\nu}$ decay

Michal Zamkovský[a] **and the NA62 Collaboration**[b]

[a] *Speaker, UCLouvain, Place de l'Université 1, Louvain-la-Neuve, Belgium, michal.zamkovsky@cern.ch*

[b] *R. Aliberti, F. Ambrosino, R. Ammendola, B. Angelucci, A. Antonelli, G. Anzivino, R. Arcidiacono, T. Bache, A. Baeva, D. Baigarashev, M. Barbanera, J. Bernhard, A. Biagioni, L. Bician, C. Biino, A. Bizzeti, T. Blazek, B. BlochDevaux, V. Bonaiuto, M. Boretto, M. Bragadireanu, D. Britton, F. Brizioli, M.B. Brunetti, D. Bryman, F. Bucci, T. Capussela, J. Carmignani, A. Ceccucci, P. Cenci, V. Cerny, C. Cerri, B. Checcucci, A. Conovaloff, P. Cooper, E. Cortina Gil, M. Corvino, F. Costantini, A. Cotta Ramusino, D. Coward, G. D'Agostini, J. Dainton, P. Dalpiaz, H. Danielsson, N. De Simone, D. Di Filippo, L. Di Lella, N. Doble, B. Dobrich, F. Duval, V. Duk, D. Emelyanov, J. Engelfried, T. Enik, N. Estrada-Tristan, V. Falaleev, R. Fantechi, V. Fascianelli, L. Federici, S. Fedotov, A. Filippi, M. Fiorini, J. Fry, J. Fu, A. Fucci, L. Fulton, E. Gamberini, L. Gatignon, G. Georgiev, S. Ghinescu, A. Gianoli, M. Giorgi, S. Giudici, F. Gonnella, E. Goudzovski, C. Graham, R. Guida, E. Gushchin, F. Hahn, H. Heath, J. Henshaw, E.B. Holzer, T. Husek, O. Hutanu, D. Hutchcroft, L. Iacobuzio, E. Iacopini, E. Imbergamo, B. Jenninger, J. Jerhot, R.W. Jones, K. Kampf, V. Kekelidze, S. Kholodenko, G. Khoriauli, A. Khotyantsev, A. Kleimenova, A. Korotkova, M. Koval, V. Kozhuharov, Z. Kucerova, Y. Kudenko, J. Kunze, V. Kurochka, V. Kurshetsov, G. Lanfranchi, G. Lamanna, E. Lari, G. Latino, P. Laycock, C. Lazzeroni, M. Lenti, G. Lehmann Miotto, E. Leonardi, P. Lichard, L. Litov, R. Lollini, D. Lomidze, A. Lonardo, P. Lubrano, M. Lupi, N. Lurkin, D. Madigozhin, I. Mannelli, A. Mapelli, F. Marchetto, R. Marchevski, S. Martellotti, P. Massarotti, K. Massri, E. Maurice, M. Medvedeva, A. Mefodev, E. Menichetti, E. Migliore, E. Minucci, M. Mirra, M. Misheva, N. Molokanova, M. Moulson, S. Movchan, M. Napolitano, I. Neri, F. Newson, A. Norton, M. Noy, T. Numao, V. Obraztsov, A. Ostankov, S. Padolski, R. Page, V. Palladino, A. Parenti, C. Parkinson, E. Pedreschi, M. Pepe, M. Perrin-Terrin, L. Peruzzo, P. Petrov, Y. Petrov, F. Petrucci, R. Piandani, M. Piccini, J. Pinzino, I. Polenkevich, L. Pontisso, Yu. Potrebenikov, D. Protopopescu, M. Raggi, A. Romano, P. Rubin, G. Ruggiero, V. Ryjov, A. Salamon, C. Santoni, G. Saracino, F. Sargeni, S. Schuchmann, V. Semenov, A. Sergi, A. Shaikhiev, S. Shkarovskiy, D. Soldi, V. Sugonyaev, M. Sozzi, T. Spadaro, F. Spinella, A. Sturgess, J. Swallow, S. Trilov, P. Valente, B. Velghe, S. Venditti, P. Vicini, R. Volpe, M. Vormstein, H. Wahl, R. Wanke, B. Wrona, O. Yushchenko, M. Zamkovsky, A. Zinchenko.*

The decay $K^+ \to \pi^+ \nu\bar{\nu}$, with a very precisely predicted branching ratio of less than 10^{-10}, is among the best processes to reveal indirect effects of new physics. The NA62 experiment at CERN SPS is designed to study the $K^+ \to \pi^+ \nu\bar{\nu}$ decay and to measure its branching ratio using a decay-in-flight technique. NA62 took data in 2016, 2017 and 2018, reaching the sensitivity of the Standard Model for the $K^+ \to \pi^+ \nu\bar{\nu}$ decay by the analysis of the 2016 and 2017 data, and providing the most precise measurement of the branching ratio to date by the analysis of the 2018 data. This measurement is also used to set limits on BR($K^+ \to \pi^+ X$), where X is a scalar or pseudo-scalar particle. The final result of the BR($K^+ \to \pi^+ \nu\bar{\nu}$) measurement and its interpretation in terms of the $K^+ \to \pi^+ X$ decay from the analysis of the full 2016-2018 data set is presented, and future plans and prospects are reviewed.

7th Symposium on Prospects in the Physics of Discrete Symmetries (DISCRETE 2020-2021)
29th November - 3rd December 2021
Bergen, Norway

PoS(DISCRETE2020-2021)070

1. Introduction

The $K^+ \to \pi^+ \nu\bar{\nu}$ is a flavor-changing neutral current decay that is theoretically very clean and extremely rare. Using the value of the tree-level elements of the CKM matrix as external inputs, the Standard Model (SM) predicts the branching ratio (BR) to be $(8.4 \pm 1.0) \times 10^{-10}$ [1]. Its theoretical origin is dominated by the short distance contribution without hadronic uncertainties as the hadronic matrix elements are extracted from the well-known decay $K^+ \to \pi^0 e^+ \nu$, corrected for the isospin-breaking and non-perturbative effects calculated in [2–4]. The $K^+ \to \pi^+ \nu\bar{\nu}$ decay is very sensitive to physics beyond the SM (BSM), probing the highest mass scales among the rare meson decays. Large deviations from the predicted BR are expected in several BSM scenarios [5].

Before the NA62, experiments E787 and E949 at Brookhaven National Laboratory measured the BR of the $K^+ \to \pi^+ \nu\bar{\nu}$ decay to be $(17.3^{+11.5}_{-10.5}) \times 10^{-11}$ [6].

The NA62 experiment uses protons from the CERN SPS accelerator, which after hitting the target produce a secondary hadron beam at a nominal momentum of 75 GeV/c and 1% momentum spread (rms). The nominal beam intensity is 750 MHz of particles, of which about 6% are kaons. The kaons are tagged by the differential Cherenkov counter (KTAG) and the beam momentum is measured by three silicon pixel spectrometer stations (GTK). A Charged Anti-counter detector suppresses products of inelastic interactions in the last GTK station, which is followed by a 110 m long vacuum tank with four tracking stations of the magnetic spectrometer. The first 60 m of vacuum define the fiducial volume (FV), where about 13% of the K^+ decay. A set of calorimeters within the vacuum tube (LAV) and in the forward direction (LKr, IRC, SAC) provide a hermetic veto for photons emitted in the K^+ decays for a polar angle up to 50 mrad. A Ring-Imaging Cherenkov counter (RICH) for the particle identification (PID) and two plastic scintillator charged hodoscopes (CHOD) are located downstream of the vacuum tank. For a further PID, two hadronic calorimeters (MUV1, MUV2) and a muon veto detector (MUV3) follow the LKr. Additional counters installed at optimized locations (HASC, MUV0) provide a hermetic coverage for charged particles produced in multi-track kaon decays. The schematic layout of the detector is shown in Fig. 1 and the full detector description can be found in [7].

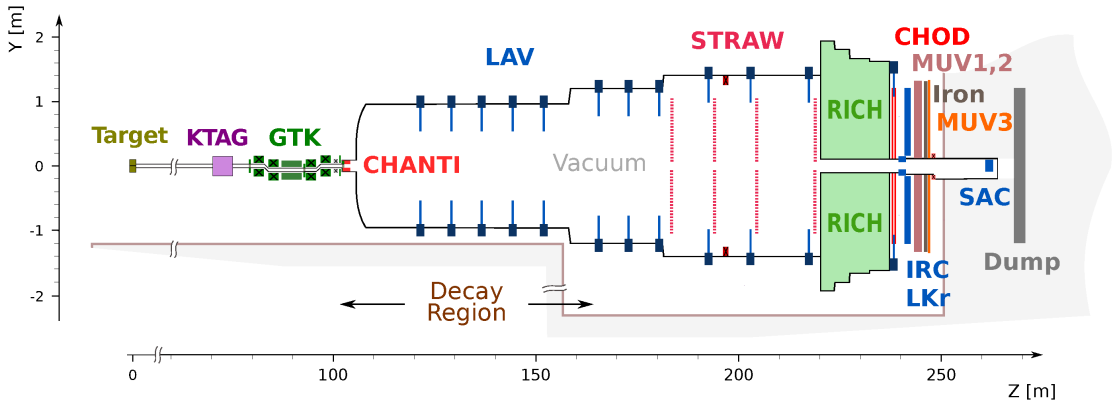

Figure 1: Schematic side view of the NA62 experiment.

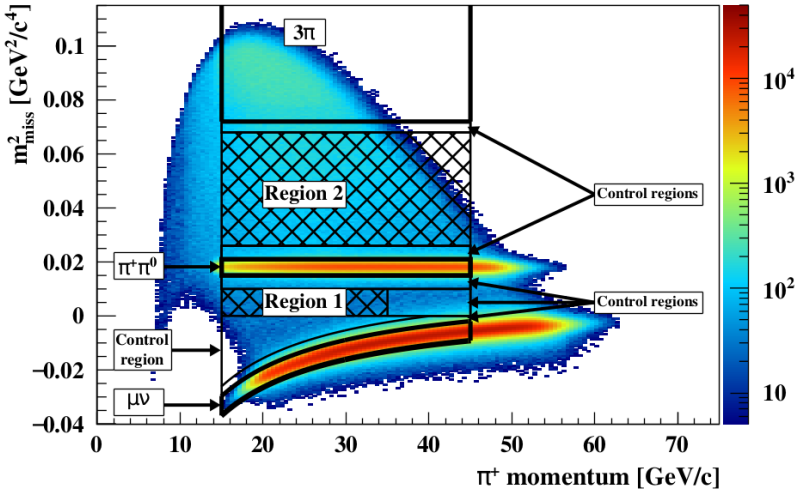

Figure 2: Reconstructed m^2_{miss} as a function of the π^+ momentum from a control data sample, before applying particle identification cuts and photon rejection, assuming the K^+ and π^+ mass for the parent and decay particle, respectively. Two signal regions (hatched areas) and control regions are shown.

2. $K^+ \to \pi^+\nu\bar{\nu}$ analysis

The event selection varies, depending on the year when the data were collected. A detailed description of event selection of 2016 and 2017 data can be found in [8, 9]. In what follows, the 2018 data set analysis is described.

The squared missing mass calculated from an upstream K^+ 4-momentum p_K and a downstream π^+ 4-momentum p_π ($m^2_{miss} = (p_K - p_\pi)^2$) is used to discriminate kinematically the main K^+ decay modes from the signal. Based on the m^2_{miss} spectrum, two signal regions on either side of the $K^+ \to \pi^+\pi^0$ peak are defined. The distribution of m^2_{miss} as a function of the pion momentum, p_{π^+}, from a control data sample showing the signal regions is depicted in Fig. 2. The signal events must have the p_{π^+} in the (15,35) GeV/c and in the (15,45) GeV/c range for regions 1 and 2, respectively.

The data set collected in 2018 is divided into two subsets, S1 and S2, which correspond to the periods before (20% of the data set) and after (80% of the data set) the installation of the new final collimator COL. The subset S2 is further divided into six categories corresponding to 5 GeV/c bins of p_{π^+}, in the range 15-45 GeV/c. The subset S1 is considered as a separate category and it is integrated over the p_{π^+} due to its small size. Dedicated criteria are applied to each category, which improves the signal sensitivity.

Kinematic selection is not powerful enough to separate the signal from the background events, therefore an additional background suppression by π^+ identification, photon and multiplicity rejection is required. The particle identification is based on the RICH measurement and a multivariate analysis of calorimetric information from the LKr, MUV1 and MUV2, with MUV3 information used as veto. The photon rejection requires no in-time activity in any of the LAV, IRC, SAC and no additional clusters in the LKr beyond 100 mm radius around the π^+ impact point. Multiplicity rejection criteria against multi-charged particles and photons interacting in the detector material

upstream of the LKr include: no in-time activity in the hodoscopes unrelated to the π^+ but in spatial coincidence with an energy deposit of at least 40 MeV in the LKr; no additional segments reconstructed in the magnetic spectrometer compatible with the decay vertex; no in-time signals in HASC and MUV0; less than four extra signals in the hodoscope in time with the π^+. The fraction of events left after applying the photon and multiplicity rejection is measured to be $\varepsilon_{RV} = 0.66 \pm 0.01$. the photon and multiplicity rejection is also effective against $K^+ \to \pi^+\pi^+\pi^-$ and $K^+ \to \pi^+\pi^- e^+\nu$ backgrounds.

The measurement of BR($K^+ \to \pi^+\nu\bar{\nu}$) relies on the calculation of the single event sensitivity (SES) and the background evaluation for each category. The SES is defined as $1/(N_{K^+} \cdot \varepsilon_{\pi\nu\bar{\nu}})$, where N_{K^+} is the effective number of K^+ decays in the FV, obtained from the normalization $K^+ \to \pi^+\pi^0$ decays, and $\varepsilon_{\pi\nu\bar{\nu}}$ is the signal selection efficiency taking into account the selection acceptance, trigger efficiency and photon plus multiplicity rejection inefficiency. The resulting SES values, and the corresponding numbers of expected SM $K^+ \to \pi^+\nu\bar{\nu}$ events for the S1 and S2 subsets, integrated over π^+, are summarized in Table 1.

	S1	S2
SES	$(0.54 \pm 0.04) \times 10^{-10}$	$(0.14 \pm 0.01) \times 10^{-10}$
$N^{exp}_{\pi\nu\bar{\nu}}$	$1.56 \pm 0.10 \pm 0.19_{ext}$	$6.02 \pm 0.39 \pm 0.72_{ext}$

Table 1: Single event sensitivities and numbers of expected SM signal events in the S1 and S2 subsets of 2018 data.

The uncertainties comprise of the systematic effects and the external error refers to uncertainties of the SM parameters.

3. Background evaluation

Background from the K^+ decays in the FV is mainly due to $K^+ \to \pi^+\pi^0(\gamma)$, $K^+ \to \mu^+\nu(\gamma)$, $K^+ \to \pi^+\pi^+\pi^-$ and $K^+ \to \pi^+\pi^- e^+\nu$ decays. Other kaon decays give a negligible contribution, estimated to be $O(10^{-2})$. All backgrounds from K^+ decays, but $K^+ \to \pi^+\pi^- e^+\nu$, are evaluated using data. The upstream backgrounds are due to the pions originating upstream of the FV. They are produced in K^+ decays between the GTK stations 2 and 3, matching an accidental beam particle and in K^+ interactions with the beam line material, either promptly or as a decay product of a neutral kaon matched to an in-time K^+. The upstream backgrounds are evaluated using a data-driven approach.

The background prediction for the sum of all contributions described above is validated in the six control regions located between the signal and the $\pi^+\pi^0$, $\mu\nu$ and 3π regions.

After unmasking the control regions the observed and expected numbers of events are found to be statistically compatible across all control regions. A summary of the background estimates summed over Region 1 and Region 2 is presented in Table 2 for two subsets S1 and S2 of the 2018 data.

Background source	Subset S1	Subset S2
$\pi^+\pi^0$	0.23 ± 0.02	0.52 ± 0.05
$\mu^+\nu$	0.19 ± 0.06	0.45 ± 0.06
$\pi^+\pi^-e^+\nu$	0.10 ± 0.03	0.41 ± 0.10
$\pi^+\pi^+\pi^-$	0.05 ± 0.02	0.17 ± 0.08
$\pi^+\gamma\gamma$	< 0.01	< 0.01
$\pi^0\ell^+\nu$	< 0.001	< 0.001
Upstream	$0.54^{+0.39}_{-0.21}$	$2.76^{+0.90}_{-0.70}$
Total	$1.11^{+0.40}_{-0.22}$	$4.31^{+0.91}_{-0.72}$

Table 2: Summary of expected numbers of background events summed over Regions 1 and 2 in the 2018 subsets.

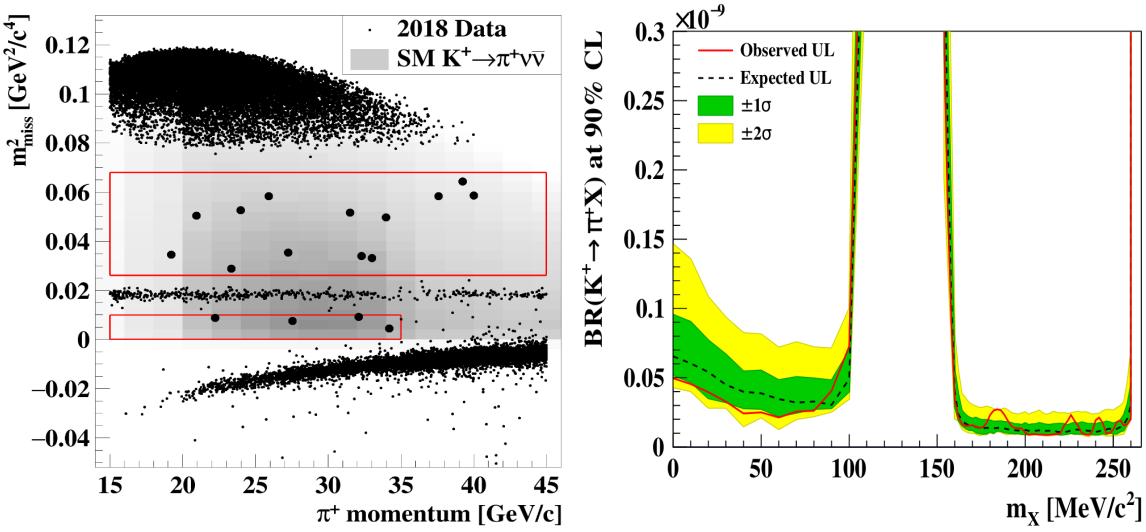

Figure 3: Left: Reconstructed m^2_{miss} as a function of p_{π^+} for events satisfying the $K^+ \to \pi^+\nu\bar{\nu}$ selection criteria. The intensity of the grey shaded area reflects the variation of the SM signal acceptance in the plane. The two boxes represent the signal regions. The events observed in Regions 1 and 2 are shown together with the events found in the background and control regions. **Right:** Upper limits on BR($K^+ \to \pi^+X$) for each tested m_X hypothesis, as obtained for the full 2016-2018 data set.

4. Results

After unmasking the signal regions, four events are found in Region 1 and thirteen in Region 2, as shown in Figure 3, Left.

A background-only hypothesis test is performed using as a test statistic the likelihood ratio for independent Poisson-distributed variables as prescribed in [10]. A p-value of 3.4×10^{-4} is obtained, corresponding to a signal significance of 3.4 standard deviations.

The combined result on the branching ratio from NA62 run 1 (data samples from 2016-2018) is:

$$BR(K^+ \to \pi^+\nu\bar{\nu}) = (10.6^{+4.0}_{-3.4}|_{stat} \pm 0.9_{syst}) \times 10^{-11}$$

at 68% CL [11], which is compatible with the predicted SM value. The first uncertainty is statistical, related to the Poissonian fluctuation of the numbers of observed events and expected background, while the second is systematic, resulting from the uncertainty in the signal and background estimates. This result is the most precise measurement of the $K^+ \to \pi^+\nu\bar{\nu}$ decay rate to date and provides the strongest evidence so far for the existence of this extremely rare process.

In several BSM scenarios a new feebly interacting scalar or pseudo-scalar particle X is foreseen. If it lives long enough to decay out of the detector or decays to invisible particles the signature of $K^+ \to \pi^+ X$ in the detectors will be the same as of $K^+ \to \pi^+\nu\bar{\nu}$ decay. As the new particle X would come from the two-body decay, it will present itself as a peak in the reconstructed m^2_{miss} distribution, centered around its invariant mass m^2_X. A peak search for m_X masses in the ranges 0-110 MeV/c^2 and 160-260 MeV/c^2 has been performed and the upper limits on the branching ratio have been set to $3-6\times10^{-11}$ and 1×10^{-11} at 90% CL, respectively. Results are displayed in Figure 3, right for a stable or invisibly decaying particle X.

5. Future plans

Since the restart of data taking in 2021, NA62 has implemented several improvements. To further mitigate the upstream backgrounds, the beam line was re-arranged to swipe away upstream π^+, a fourth GTK station was added and a new veto-counter system to detect upstream decay products was installed. An additional off-axis calorimeter (HASC-2) was placed next to HASC to further suppress $K^+ \to \pi^+\pi^0$ background. The NA62 experiment also runs at a higher intensity to reach its goal of BR($K^+ \to \pi^+\nu\bar{\nu}$) measurement with $O(10)$ statistical precision in the coming years.

References

[1] A. J. Buras, D. Buttazzo, J. Girrbach-Noe and R. Knegjens, JHEP **11**, 033 (2015).

[2] J. Brod, M. Gorbahn and E. Stamou, Phys. Rev. D **83**, 034030 (2011).

[3] G. Isidori, F. Mescia and C. Smith, Nucl. Phys. B **718**, 319 (2005).

[4] F. Mescia and C. Smith, Phys. Rev. D **76**, 034017 (2007).

[5] M. Blanke, A. J. Buras and S. Recksiegel, Eur. Phys. J. C **76**, 182 (2016).

[6] A.V. Artamonov *et al.*, Phys. Rev. D **79**, 092004 (2009).

[7] E. Cortina Gil *et al.* [NA62 Collaboration], JINST **12**, P05025 (2017).

[8] E. Cortina Gil *et al.* [NA62 Collaboration], Phys. Lett. B **791**, 156-166 (2019).

[9] E. Cortina Gil *et al.* [NA62 Collaboration], JHEP **11**, 042 (2020).

[10] P.A. Zyla *et al.* [PDG], Prog. Theor. Exp. Phys., 083C01 (2020).

[11] E. Cortina Gil *et al.* [NA62 Collaboration], JHEP **06**, 093 (2021).